Eng. Sci., 2025, **38**, 1951

Engineered Science
DOI: https://dx.doi.org/10.30919/es1951

Multi-Time-Scale Optimized Operation Strategies for Integrated Energy Systems Considering Energy Efficiency Levels and Equipment Safety Risks

Zhenlan Dou,[1] Chunyan Zhang,[1] Songcen Wang,[3] Limin Hong,[4] Yingying Mao[5] and Dejian Yang[2,*]

Abstract

As the process of energy transition progresses, the integrated energy system (IES), as a key carrier for achieving carbon neutrality, faces the challenge of balancing energy efficiency improvements with equipment safety risks in its optimized operation. At the same time, IES consolidate diverse energy streams such as electrical power, thermal energy, and gaseous fuels. Nevertheless, the inherent intermittency of renewable energy sources often results in equipment overloading or accelerated degradation, making it challenging for traditional single-time-scale optimization to balance economic and safety considerations. This paper focuses on multi-time scale optimization strategies. Specifically, first, the energy efficiency-safety collaborative evaluation index is introduced to combine energy utilization rate with risk probability quantification; Secondly, a dynamic safety constraint model is developed to modify the operational limits in real-time according to equipment status. Lastly, a rolling optimization algorithm combining day-ahead planning, intraday adjustments, and real-time feedback is proposed to enhance system adaptability. The experiment uses actual IES data from a specific region. Results show that compared to the benchmark, the new strategy increases system energy efficiency by 12.8% (from 85% to 97.8%), reduces equipment safety risks by 15.3% (from 10% to 8.47%), and achieves a 14.5% energy cost saving and 96.2% reliability. These data verify the effectiveness of the strategy and provide support for the robust operation of IES.

Keywords: Integrated energy system; Energy efficiency level; Equipment safety risk; Multi-time scale optimization; Evaluation indicators.
Received: 16 October 2025; Revised: 04 December 2025; Accepted: 13 December 2025
Article Type: Research article.

1. Introduction

As global energy demand rises and environmental issues intensify, optimal operation strategies for integrated energy systems have garnered significant attention from both academia and industry.[1] These systems enhance overall efficiency and reliability by integrating various energy forms (*e.g.*, electricity, heat, and gas) and enabling efficient energy use and multi-energy complementarity.[2] However, traditional optimization strategies for integrated energy systems[3-6] typically focus on energy dispatch at a single time scale, neglecting the complexity and dynamic nature of system operations across multiple time scales. This approach struggles to meet the diverse needs of modern integrated energy systems, especially in improving energy efficiency and managing equipment safety risks.[7] Traditional single-time scale optimization strategies, by ignoring the volatility of renewable energy output, are prone to equipment overload and increased operating costs, making it difficult to achieve a balance between energy efficiency and safety. This paper draws on this perspective and introduces multi-timescale optimization to overcome the shortcomings of traditional strategies and improve the overall system performance.

Energy efficiency is a crucial metric for evaluating the performance of integrated energy systems. Amid the growing scarcity of energy resources, improving energy efficiency not only helps reduce energy costs but also lowers greenhouse gas emissions, which is of great significance in achieving sustainable development goals. However, the energy efficiency improvement of integrated energy systems is not achieved overnight, but requires collaborative optimization on multiple time scales.[8] In the short term, real-time optimal scheduling can quickly adjust energy distribution according to immediate energy demand and equipment status, ensuring the

[1,#]*State Grid Shanghai Municipal Electric Power Company, Shanghai, 200122, China*
[2,#]*Northeast Electric Power University, Jilin, 132012, China*
[3]*China Electric Power Research Institute, Beijing, 100192, China*
[4]*School of Information Engineering, Nanchang University, Nanchang, 330031, China*

efficient operation of the system.[9] In the medium and long term, optimization in the planning and design stages must consider the life cycle of equipment, fluctuations in the energy market, and changes in policies and regulations to achieve long-term energy efficiency improvements in the system.[10] At the same time, equipment safety risks are a crucial factor that cannot be overlooked during the operation of integrated energy systems. The safe operation of equipment is directly related to the stability and reliability of the system. Once it fails, it will not only lead to an interruption of the energy supply but also result in serious safety accidents. Therefore, when optimizing the operation strategy, the assessment and control of equipment safety risks must be fully considered. The management of equipment safety risks requires comprehensive consideration on multiple time scales, including real-time monitoring and early warning, the preventive maintenance plans, and the improvement of emergency response mechanisms. By incorporating energy efficiency levels and equipment safety risks into the multi-time-scale optimized operation strategy of integrated energy systems, a balance can be achieved between system efficiency and safety.

In recent years, multi-time-scale optimization methods have gained significant attention in energy systems. By segmenting system operations into short-term, medium-term, and long-term levels and optimizing decisions at each level, this method achieves comprehensive system optimization. It effectively adapts to the dynamic nature of energy systems, enhancing flexibility and adaptability. Implementing such a strategy in integrated energy systems necessitates considering factors like energy demand forecasts, equipment characteristics, energy market price volatility, and regulatory constraints. A multi-time-scale optimization model can collaboratively optimize energy production, transmission, and consumption across different timescales, improving efficiency and reducing safety risks. Advanced information and control technologies, such as the Internet of Things, big data, and artificial intelligence, provide the necessary foundation for realizing multi-time-scale optimization in integrated energy systems.[11] By collecting and analyzing system operation data in real-time, accurate predictions of energy demand and real-time monitoring of equipment status can be achieved, thus providing strong support for informed decision-making. Meanwhile, advanced control technologies like model predictive control facilitate dynamic adjustments and optimal control of system operations, thereby enhancing operational efficiency and safety.[12]

In the study of multi-time-scale optimal operation strategies for integrated energy systems, balancing energy efficiency and equipment safety risks is essential for efficient and safe operation.[13] Enhancing energy efficiency involves optimizing energy production, transmission, and consumption processes. Meanwhile, managing equipment safety risks requires effective measures during operation, maintenance, and management.[14] For short-term optimization, real-time monitoring and adjustment of energy distribution ensure efficient and safe system operation.[15] In medium-term optimization, a well-planned maintenance schedule and energy management strategy can extend equipment life and boost energy efficiency. Long-term optimization focuses on equipment upgrades and energy market trends to ensure system sustainability. Thus, multi-time-scale strategies must balance energy efficiency and safety risks to achieve optimal system performance.

Overall, in this model, IoT technology is used for real-time data acquisition and equipment monitoring, big data technology processes historical load and renewable energy data to support forecasting, and artificial intelligence technology (such as deep learning) is applied to the training and adaptive adjustment of optimization algorithms, thereby achieving a dynamic balance between energy efficiency and safety. research on multi-time-scale optimal operation strategies for integrated energy systems holds significant theoretical and practical value. Integrating energy efficiency and safety risk considerations into these strategies enables efficient and safe operation across multiple timescales, thereby supporting the sustainable development of integrated energy systems.

2. Related work

2.1 Theoretical basis for multi-time-scale optimization of integrated energy systems

The theoretical foundation of multi-time-scale optimization for IES is vital for ensuring the efficient and reliable operation of energy systems.[16] This theoretical basis encompasses multiple disciplines, including operations research, control theory, economics, and energy engineering,[17] and seeks to achieve optimal scheduling of energy systems across various time scales through mathematical modeling and optimization algorithms.[18]

Multi-time scale optimization models need to consider energy demand and supply characteristics at different time scales. Day-ahead optimization is primarily based on 24-hour forecast data for scheduling plans. Intraday optimization adjusts the day-ahead plan according to the actual operational situation, and real-time optimization dynamically adjusts the system at the minute level.[19] These optimizations on different time scales are interrelated and together ensure the economy and reliability of the system.

When establishing a multi-time-scale optimization model, the setting of the objective function is one of the core problems. The objective functions of this paper include equipment operating costs, maintenance costs and energy procurement costs. Among them, the operating cost of the equipment is

[5]*Siping Power Supply Company, State Grid Jilin Electric Power Co., Ltd., Siping, 136000, China*

[#]*State Grid Shanghai Municipal Electric Power Company and Northeast Electric Power University contributed equally to this work.*

[*]*Email:* Ydjian1015@163.com (D. Yang)

mainly determined by the power loss and operating time of the equipment, and the calculation process is shown in Eq. (1):

$$C_{\text{operation}} = \sum_{i=1}^{N} P_i \times t_i \times C_{\text{unit}} \quad (1)$$

where P_i is the power loss of the equipment, t_i is the running time of the equipment, and C_{unit} is the cost per unit power loss. The maintenance cost is calculated according to the maintenance cycle and maintenance cost of the equipment, and the calculation process is shown in Eq. (2):

$$C_{\text{maintenance}} = \sum_{i=1}^{N} \frac{C_{\text{maintenance},i}}{T_{\text{maintenance},i}} \times t_i \quad (2)$$

Among them, $C_{\text{maintenance},i}$ is the single maintenance cost of the equipment, and $T_{\text{maintenance},i}$ is the maintenance period of the equipment. The energy procurement cost is calculated according to the market price and purchase volume of energy, and its calculation process is shown in Eq. (3):

$$C_{\text{procurement}} = \sum_{j=1}^{M} E_j \times P_{\text{market},j} \quad (3)$$

Among them, E_j is the amount of energy purchased and $P_{market,j}$ is the market j price of energy.

Generally, the objective function encompasses multiple objectives, including cost minimization, energy efficiency maximization, and risk minimization. The cost minimization objective can be expressed by Eq. (4):

$$\min C = \sum_{t=1}^{T} \left(c_{\text{gen}} \cdot P_{\text{gen},t} + c_{\text{stor}} \cdot P_{\text{stor},t} + c_{\text{grid}} \cdot P_{\text{grid},t} \right) \quad (4)$$

Among them, $c_{gen,t}$, $c_{stor,t}$, and $c_{grid,t}$ represent the cost coefficients of power generation, energy storage and power purchase at time t, respectively, and $P_{gen,t}$, $P_{stor,t}$ and $P_{grid,t}$ represent the power generation, energy storage and power purchase at time t, respectively.

The goal of maximizing energy efficiency can be achieved by improving energy utilization, and its calculation process can be expressed by Eq. (5):

$$\max E_{\text{eff}} = \frac{\sum_{t=1}^{T} P_{\text{load},t}}{\sum_{t=1}^{T} \left(P_{\text{gen},t} + P_{\text{stor},t} + P_{\text{grid},t} \right)} \quad (5)$$

where E_{eff} denotes the energy efficiency and $P_{\text{load},t}$ denotes the load demand at time t.

The risk minimization goal needs to consider the safe operation of the equipment and the reliability of the system, and its calculation process can be expressed by Eq. (6):

$$\min R = \sum_{t=1}^{T} \left(r_{\text{fail}} \cdot \mathbb{I}(P_{\text{fail},t}) + r_{\text{outage}} \cdot \mathbb{I}(P_{\text{outage},t}) \right) \quad (6)$$

Among them, r_{fail} and r_{outage} represent the risk costs of equipment failure and system power failure, respectively, and $\mathbb{I}$ is an indicator function, which takes the value of 1 when either equipment failure or system power failure occurs, and otherwise, it is 0.

Advanced optimization algorithms, such as linear programming, mixed-integer linear programming, particle swarm optimization, and genetic algorithms, are commonly employed to solve multi-time-scale optimization models. These algorithms can identify the optimal or near-optimal solutions for the objective function, given that the constraints are met.

To enhance the adaptability and accuracy of the optimization models, uncertainties and dynamics must be considered. For instance, forecasting errors in renewable energy output and load can affect optimization outcomes. Therefore, robust optimization and stochastic optimization are widely used in multi-time-scale models to improve their robustness and adaptability.

2.2 Energy efficiency improvement strategies in integrated energy systems

In integrated energy systems, energy efficiency enhancement strategies are essential for achieving optimal operation and sustainable development.[20] Energy efficiency improvement can not only reduce energy consumption and operating costs, but also reduce greenhouse gas emissions, which is of great significance to environmental protection.[21-23] This paper will discuss energy efficiency improvement strategies in integrated energy systems from a theoretical perspective.[24]

Firstly, the energy efficiency improvement strategy should account for the overall characteristics of the energy system, including the interaction and conversion among different energy forms such as electricity, heat, and cooling.[25] In this system, the key to improving energy efficiency lies in optimizing the production, transmission, storage, and consumption processes of energy. Through reasonable scheduling and control, the energy utilization rate can be improved and the energy loss can be reduced.[26]

In theoretical terms, energy efficiency is commonly assessed by energy utilization, defined as the ratio of output energy to input energy in the system. The calculation process of the energy utilization rate is shown in Eq. (7):

$$\eta = \frac{E_{\text{out}}}{E_{\text{in}}} \quad (7)$$

where E_{out} represents the total energy output by the system and E_{in} represents the total energy input by the system. Improving energy efficiency means that the system can provide more output energy with the same input energy, or reduce the input energy while maintaining the same output energy.

Energy efficiency improvement strategies need to consider the dynamic characteristics and uncertainties of the system. In an integrated energy system, both energy demand and supply can change over time and are influenced by various factors, including weather changes and market price fluctuations.[27]

Therefore, energy efficiency improvement strategies need to have certain flexibility and adaptability to cope with these dynamic changes and uncertainties.[28] Dynamic programming is a commonly used method that optimizes the system's operation strategy by establishing a multi-stage decision model. The basic idea of dynamic programming is to decompose the problem into multiple stages, where each stage makes an optimal decision, thereby achieving the optimal operation of the entire system. The mathematical model of dynamic programming can be expressed as Eq. (8):

$$V_t = \max_{a_t}\{R_t(a_t) + \beta V_{t+1}\} \quad (8)$$

Among them, V_t represents the system value at time t, a_t represents the decision variable at time t, $R_t(a_t)$ represents the immediate return obtained by taking decision a_t at time t, and β is the discount factor, which represents the current value of the future return.

At the same time, energy efficiency improvement strategies must also consider system integration and coordination. In the integrated energy system, there are mutual influences and restrictions among different energy forms.[29] For example, energy integration and conversion can be achieved between power systems and thermal systems through combined heat and power (CHP) systems. By optimizing these integration and conversion processes, energy utilization efficiency can be improved. The integrated optimization model usually needs to consider the coupling relationship and conversion efficiency of multiple energy forms, and its mathematical model can be expressed as Eq. (9-10):

$$\min \sum_{t=1}^{T}\left(c_{\text{elec}} \cdot P_{\text{elec},t} + c_{\text{heat}} \cdot Q_{\text{heat},t}\right) \quad (9)$$

$$s.t.\, P_{\text{elec},t} = \eta_{\text{CHP}} \cdot Q_{\text{heat},t} + P_{\text{grid},t} \quad (10)$$

where c_{elec} and c_{heat} represent the cost of electricity and heat, respectively, $P_{elec,t}$ and $Q_{heat,t}$ represent the electricity and heat demand at time t, respectively, ηCHP represents the conversion efficiency of cogeneration, and $P_{grid,t}$ represents the electricity purchased from the grid.

3. Construction of our model

The time scale division in this paper is based on the operational characteristics of the Integrated Energy System (IES): day-ahead optimization uses a 24-hour cycle with a 1-hour time step to handle highly predictable loads and renewable energy output; intraday optimization uses a 1-hour cycle with a 15-minute time step to address short-term fluctuations; and real-time optimization operates on a minute-by-minute scale with a 5-minute time step to quickly respond to emergencies. The division criteria consider data availability, computational complexity, and system security requirements, ensuring synergy and complementarity among the different scales. As depicted in Fig. 1, the multi-time-scale optimization operation strategy model for the IES proposed in this paper consists of three key components: an energy efficiency-safety collaborative evaluation index, a dynamic safety constraint model, and a rolling optimization algorithm. At the same time, in order to realize the efficient operation of the system, this paper introduces a multi-time scale optimization operation strategy, which optimizes the system from three time scales: short-term (hourly level), medium-term (daily level) and long-term (monthly level). Short-term optimization focuses on real-time scheduling, medium-term optimization focuses on daily operation plans, and long-term optimization focuses on equipment maintenance and energy procurement strategies. This multi-time scale optimization strategy can effectively balance the energy efficiency level of the system and equipment safety risks. These components collectively balance system energy efficiency and equipment safety risks, thereby improving the overall operating efficiency and reliability of the system.

The energy efficiency-safety collaborative evaluation index is a core component of the model, quantifying and combining energy utilization with equipment safety risks. The index is realized by introducing a comprehensive evaluation function $E_{\text{eff-safety}}$, which is specifically calculated as shown in Eq. (11):

$$E_{\text{eff-safety}} = \alpha \cdot \eta + (1-\alpha) \cdot (1-\beta) \quad (11)$$

Among them, η represents the energy utilization rate, which reflects the ratio of the energy effectively utilized by the system per unit time to the total input energy. β represents the probability of equipment safety risk, which is obtained through real-time evaluation of the equipment's failure rate and operating status. The parameter α is a weighting factor used to balance the importance of energy efficiency and safety risks in the comprehensive evaluation. By adjusting the value of α, a flexible trade-off can be made between improving energy efficiency and reducing equipment safety risks. This evaluation index provides a comprehensive performance measurement standard for the optimization model, ensuring that the optimization process does not overlook the safety of equipment while pursuing energy efficiency improvements.

In the optimization operation strategy, the constraints considered in this paper include: equipment operation constraints, energy supply constraints and safety constraints, specifically:

(1) Equipment operation constraints ensure that the operating power of the equipment shall not exceed its rated power, and the operating time shall not exceed its maximum allowable operating time. Its calculation process is shown in Eq. (12,13):

$$P_i \le P_{\text{rated},i} \quad \forall i \in \{1,2,\dots,N\} \quad (12)$$

$$t_i \le T_{max,i} \quad \forall i \in \{1,2,\dots,N\} \quad (13)$$

(2) The energy supply constraint guarantees that the energy supply of the system must meet the energy demand, and its calculation process is shown in Eq. (14):

$$\sum_{j=1}^{M} E_j \ge E_{demand} \quad (14)$$

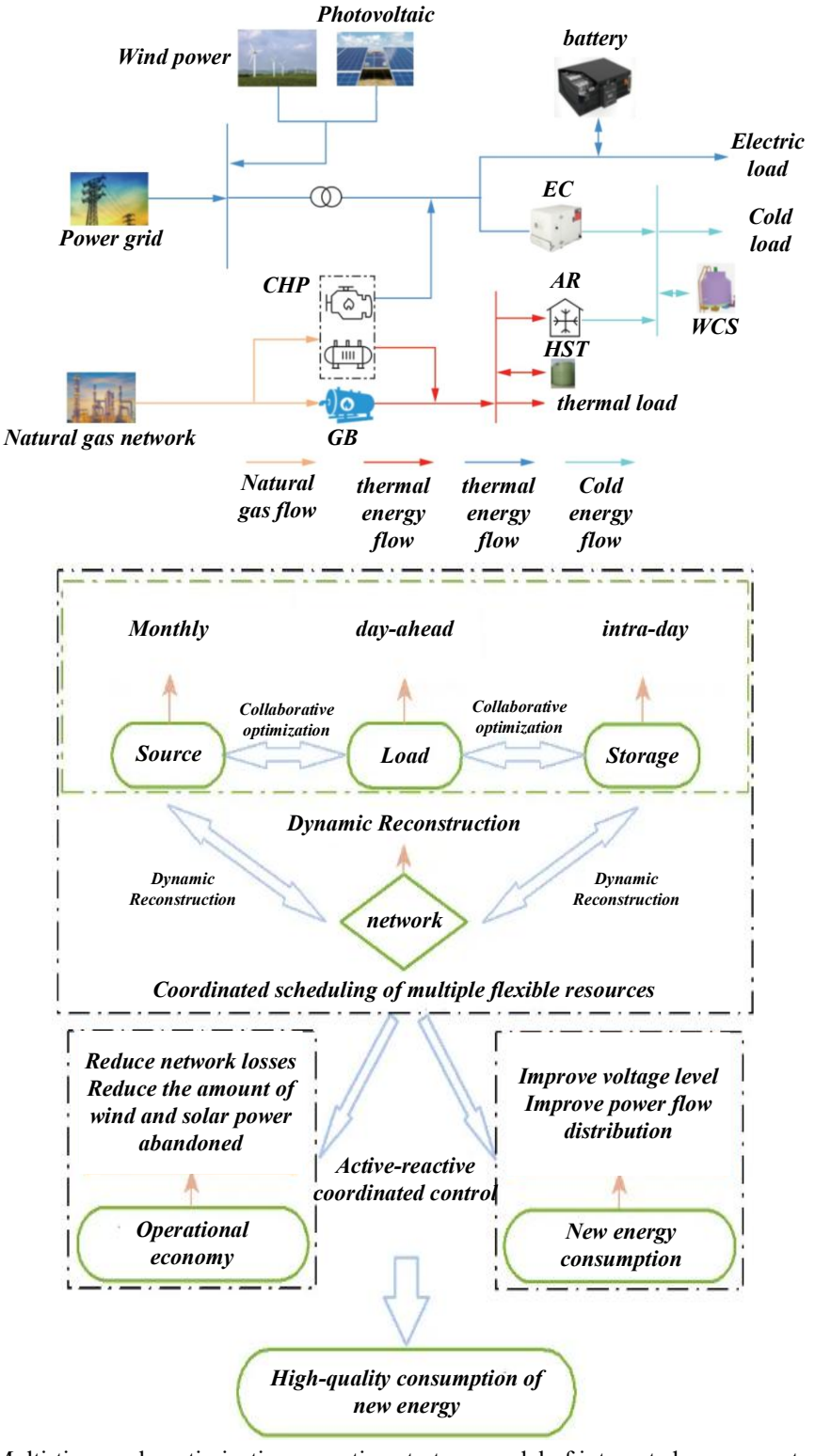

Fig. 1: Multi-time scale optimization operation strategy model of integrated energy system (IES).

(3) Safety constraints ensure that the operation of the equipment must meet safety requirements, including the temperature, pressure and other parameters of the equipment within the safe range. The calculation process is shown in Eq. (15,16):

$$T_{\text{equipment},i} \leq T_{\text{safe},i} \quad \forall i \in \{1,2,\dots,N\} \tag{15}$$

$$P_{\text{equipment},i} \leq P_{\text{safe},i} \quad \forall i \in \{1,2,\dots,N\} \tag{16}$$

In the optimization process, in order to deal with the constraint conflict problem, this paper introduces the constraint relaxation factor. The constraint relaxation factor allows the constraint condition to be violated within a certain range to avoid the solution-free problem in the optimization process. The definition of the constraint relaxation factor is

shown in Eq. (17):

$$\epsilon_i = \frac{\Delta C_i}{C_i} \tag{17}$$

where ΔC_i is the cost increase caused by violation of constraints, and C_i is the total cost of equipment. The cost increase due to violation of constraints is calculated using Eq. (18):

$$C_{penalty} = \sum_{t=1}^{T}(\lambda_{power} \cdot P_{violation,t} + \lambda_{device} \cdot D_{violation,t}) \tag{18}$$

where $P_{violation,t}$ and $D_{violation,t}$ represent the power and equipment constraint violation at time t, respectively, λ_{power} and λ_{device} are the corresponding penalty coefficients, set based on actual operating data.

In the optimization process, the constraint relaxation factor is used to deal with the conflict of equipment operation constraints and energy supply constraints. When the operating power of the equipment exceeds its rated power, the constraint relaxation factor allows it to be overloaded within a certain range, but increases the corresponding cost. The specific application is shown in Eq. (19):

$$P_i \leq P_{\text{rated},i} \times (1 + \epsilon_i) \quad \forall i \in \{1,2,\ldots,N\} \tag{19}$$

The dynamic safety constraint model is another key component of optimizing the operational strategy, and its function is to dynamically adjust the operational boundary according to the real-time state of the equipment. The model establishes the safe operation constraints of the equipment by monitoring key parameters in real-time, such as temperature, pressure, and current. Specifically, for each device i, its safe operation constraints can be expressed as Eq. (20):

$$g_i(x_i, t) \leq 0 \tag{20}$$

where x_i is the operating state variable of equipment i and t represents time. Function g_i is a constraint function defined according to the physical characteristics and safety standards of the equipment, ensuring the equipment operates within a safe range.

The rolling optimization algorithm is the key tool for realizing multi-time-scale optimization, and its design includes three levels: day-ahead planning, intraday adjustment, and real-time feedback. The algorithm ensures the system's running efficiency and adaptability at different time scales through hierarchical optimization strategies. Initially, in the day-ahead stage, the model develops the system's operation plan based on the forecasted energy demand and renewable energy generation. The plan considers the long-term operating characteristics of the equipment, as well as the price fluctuations of the energy market, and determines the start-stop plan and energy distribution scheme of the equipment by optimizing objective function $F_{\text{day-ahead}}$. The objective function usually includes objectives such as energy cost minimization and energy efficiency maximization, and its form can be expressed as Eq. (21):

$$F_{\text{day-ahead}} = \min\left(C_{\text{energy}} + \lambda \cdot (1 - E_{\text{eff-safety}})\right) \tag{21}$$

where C_{energy} is the energy cost and λ is a penalty factor used to balance the relationship between the energy cost and the energy efficiency-safety indicator.

During the intraday phase, the model revises the day-ahead plan using real-time monitoring data. The optimization objective at this stage is to accommodate the intermittency and load variations of renewable energy, and to adjust the operating status and energy distribution of the equipment by optimizing the objective function $F_{\text{intra-day}}$. The objective function takes into account the real-time operating status of equipment and short-term price fluctuations in the energy market, and its form can be expressed as Eq. (22):

$$F_{\text{intra-day}} = \min\left(C_{\text{real-time}} + \mu \cdot (1 - E_{\text{eff-safcty}})\right) \tag{22}$$

where $C_{\text{real-time}}$ is the real-time energy cost, and μ is another penalty factor used to adjust the target weight during the real-time optimization process.

Finally, in the real-time phase, the model makes immediate adjustments to system operations via a rapid feedback mechanism. The optimization goal here is to ensure both the system's instant operational efficiency and equipment safety, which is achieved by optimizing the objective function $F_{\text{real-time}}$. The objective function mainly focuses on the instant operating state and energy efficiency-safety indicators of the equipment, and its form can be expressed as Eq. (23):

$$F_{\text{real-time}} = \min\left(\nu \cdot (1 - E_{\text{eff-safety}})\right) \tag{23}$$

where ν is a real-time adjustment factor used to ensure efficient operation of the system and equipment safety under transient conditions.

4. Experiment and results analysis

4.1 Data sets and data processing

In this study, the experimental dataset is sourced from the operational data of a regional Integrated Energy System (IES), covering detailed information on electricity, heat, and gas flows, as well as equipment status, energy production and consumption, renewable energy forecasts, and failure records. To validate the model, the dataset was divided into a training set (70%), a validation set (15%), and a test set (15%) based on time series data. This division maintained the temporal continuity of the data and prevented future information leakage. The training set was used for model learning, the validation set for hyperparameter tuning, and the test set for final performance evaluation. Data preprocessing involves cleaning to remove outliers and missing values, followed by normalization to address dimensional differences in energy flow data. Additionally, fluctuation data for wind and solar outputs, generated from historical meteorological data and actual records, are added to simulate renewable energy intermittency. This preprocessing ensures high-quality data for model training and validation, supporting robust evaluation of optimization strategies.

4.2 Evaluation index

The evaluation indexes of the model primarily include the energy efficiency index, equipment safety risk rate, energy cost savings rate, and system reliability. The energy efficiency index is measured by calculating the change in the system's energy utilization rate, specifically the percentage improvement in energy efficiency after optimization compared to before optimization. The equipment safety risk rate is quantified by evaluating the change in equipment failure probability, which reflects the safety status of the equipment under the optimized operation strategy. Equipment safety risk rate is defined as the change in failure probability, and the calculation process is Eq. (24):

$$R(t) = \frac{P_{failure}(t) - P_{base}}{P_{base}} \tag{24}$$

where, $P_{failure}(t)$ is the failure probability at time t, which is calculated using the Weibull distribution model as Eq. (25):

$$P_{failure}(t) = 1 - exp(-(\frac{t}{\eta})^{\beta}) \tag{25}$$

where, η and β are equipment reliability parameters, fitted based on historical failure data.

The energy cost saving rate is determined by comparing the system's total energy costs before and after optimization, indicating the economic benefits of the strategy. System reliability is assessed by the proportion of continuous and stable operation time under the optimized strategy, reflecting overall system stability. These indicators evaluate the effectiveness and practicality of multi-time-scale optimization strategies from various angles, offering robust support and reference for the reliable operation of integrated energy systems.

4.3 Experiment-related settings

In the experiment presented in this paper, the selection of hyperparameters and the formula of the loss function are crucial in implementing multi-time-scale optimization strategies. Hyperparameter choices directly influence the model's training outcomes and optimization performance. First, for the energy efficiency-safety collaborative evaluation index, the weighting coefficient α was determined through sensitivity analysis, with an initial value of 0.5 and a recommended range of 0.3 to 0.7. The value of α was based on Pareto front analysis to balance the influence of energy efficiency and safety indicators, specifically optimized on the validation set through grid search. In the dynamic safety constraint model, the safe operation boundary of the equipment is dynamically adjusted based on real-time monitoring data, and its constraint relaxation factor, ϵ is set to 0.05 to ensure that the equipment operates within the safe range without excessively limiting the system's flexibility. In the rolling optimization algorithm, the optimization weights for day-ahead planning, intraday adjustment, and real-time feedback are denoted as $\lambda_{day-ahead} = 0.5$, $\lambda_{\text{intra-day}} = 0.3$, and $\lambda_{real-time} = 0.2$, respectively. These weights reflect the importance of different time scales in achieving the overall optimization goal. Meanwhile, the number of iterations was set to 1000, and the learning rate was set to 0.01. This setting, based on grid search and cross-validation results, ensures model convergence on the training set while avoiding overfitting. Specifically, we observed that the loss function stabilized after 1000 iterations, and the learning rate of 0.01 achieved the best balance on the validation set.

4.4 Specific experiments

It can be seen from the data in Table 1 that Experiment 3 performed best in terms of energy efficiency improvement, equipment safety risk reduction, and system reliability, achieving improvements of 12.8%, 15.3%, and 96.2%, respectively. Experiment 1 performed best in terms of energy cost savings, achieving a 13.7% reduction. Overall, the optimization strategies employed in each experiment have improved system performance to varying degrees, demonstrating the effectiveness of the integrated energy system optimization strategy.

The data in Table 2 show that the multi-time-scale optimization strategy performs best in terms of energy efficiency improvement, equipment safety risk reduction, and system reliability, with improvements of 12.8%, 15.3%, and 96.2%, respectively. In contrast, the benchmark method performed the worst on all indicators. Although single-time-scale optimization and traditional economic scheduling have improved some indicators, the overall performance is not as good as that of the multi-time-scale optimization strategy, which highlights the importance of comprehensively considering multiple time scales to improve system performance.

The left diagram in Fig. 2 illustrates the changes in power output of various energy supply methods over 24 hours. Among them, the output of wind turbines (blue) and photovoltaics (orange) fluctuates greatly, and the output of combined heat and power (CHP) units (green) and grid imports (red) remains relatively stable. The right-hand graph

Table 1: Performance comparison table of integrated energy system optimization strategies.

Experiment No.	Scenario description	Equipment operating status	Energy needs	Optimization objective
1	High load scenario	All equipment running at full load	1000 kW	Minimizing running costs
2	Medium load scenario	Some equipment is fully loaded and some equipment is running at low load	500 kW	Balance Energy Efficiency with Cost
3	Low load scenario	All equipment operates at low load	200 kW	Maximize equipment life

Table 2: Performance comparison of different optimization strategies in integrated energy systems.

Methods	Energy efficiency improvement	Equipment safety risk reduction	Energy cost savings	System reliability
Benchmark Method	8.5%	10.0%	12.0%	94.5%
Multi-time-scale optimization strategy	12.8%	15.3%	14.5%	96.2%
Single time scale optimization	9.8%	12.5%	13.2%	95.0%
Traditional economic dispatch	11.0%	14.0%	13.8%	95.5%

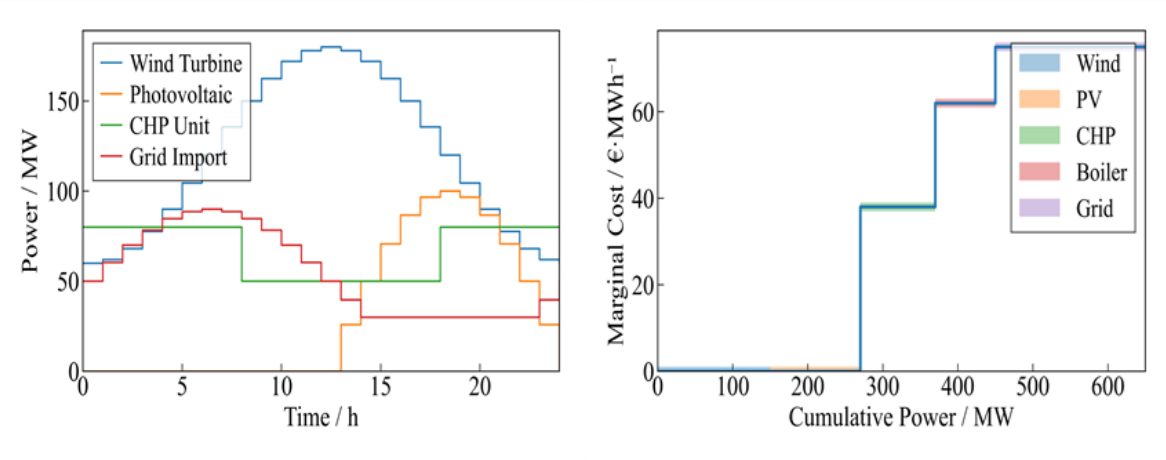

Fig. 2: Analysis of optimal operation strategy of integrated energy system.

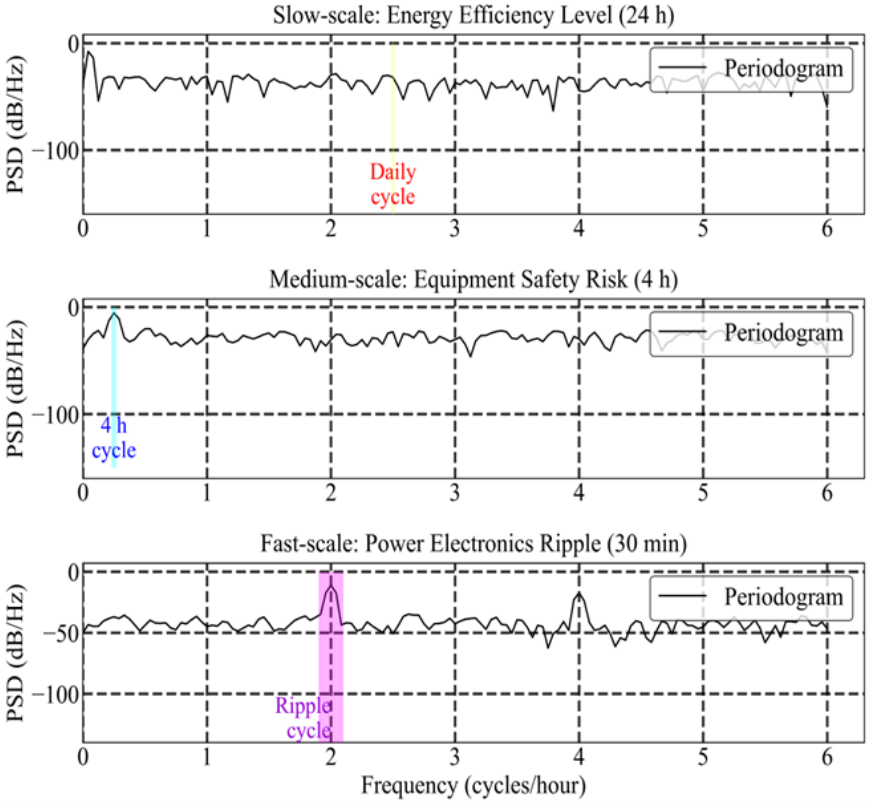

Fig. 3: Multi-scale analysis of integrated energy system.

shows the marginal costs of different energy sources relative to accumulated power, with lower costs for wind and photovoltaic (PV) and higher costs for CHP and grid imports. The results indicate that the optimized operation strategy effectively balances the stability and economic efficiency of energy supply.

In Fig. 3, the upper figure presents the power spectral density (PSD) analysis of the integrated energy system across various time scales. The first graph displays energy efficiency levels on a slow scale (24 hours), and the periodic graph reveals the effect of diurnal cycles on energy efficiency. The second graph shows equipment safety risks at a medium scale (4 hours), with 4 hours indicating moderate volatility in equipment operation. The third figure analyzes the power electronic fluctuations at the fast scale (30 minutes), particularly the fluctuation period around 2 Hz, which reflects the dynamic characteristics of power electronic devices at this scale. These analyses contribute to the understanding of the behavioral characteristics of energy systems at different time scales.

In Fig. 4, the upper graph shows the temporal variation of the risk index for the combined heat and power (CHP) system and the power grid. The CHP risk index peaks at around 0.8 at noon, whereas the power grid risk index has smaller fluctuations and reaches a maximum of about 0.6. The lower graph depicts the trends in CHP and boiler efficiency, along with total power demand. CHP efficiency reaches its highest value of approximately 0.6 at noon, while boiler efficiency peaks at around 0.9 in the afternoon. Total power demand is highest at noon and in the late evening. These data reveal the operating characteristics and risk changes of different energy systems throughout the day.

In Fig. 5, the upper graph displays the efficiencies of various energy conversion devices under day-ahead and intraday optimization, with the highest efficiency achieved by the electric boiler (EB) at 0.92. The figure below shows the efficiency under real-time optimization. The efficiency of electric boilers is still the highest at 0.90. Combined heat-and-power (CHP) and heat pump (HP) have high efficiencies under both optimizations, while power-to-gas (P2G) and combined power-to-gas (CERG) have relatively low efficiencies of 0.75 and 0.73, respectively. These data show that electric boilers perform well under different optimization strategies.

In Fig. 6, the upper graph shows the energy accumulation

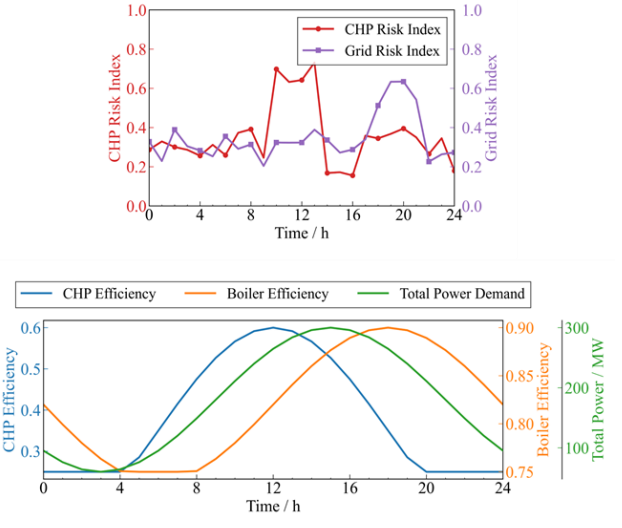

Fig. 4: Operational risk and efficiency analysis of integrated energy system.

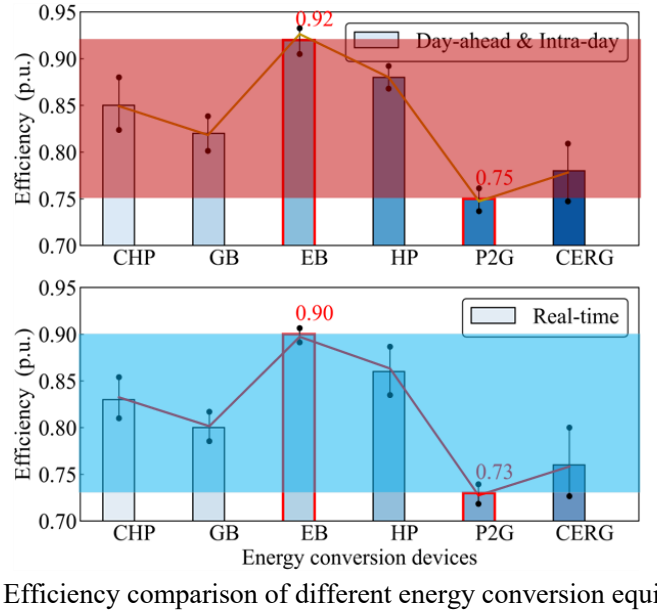

Fig. 5: Efficiency comparison of different energy conversion equipment.

of the battery at different time points, with blue representing the energy accumulation in the first step, reaching a maximum of 39,273.8 MWh and a minimum of 102.5 MWh. The lower graph shows the battery's charging status and efficiency over different time periods, with blue indicating high efficiency, gray representing medium efficiency, and red indicating low efficiency. Experimental data show that the charging status peaks at around 10 hours, while inefficient charging mainly occurs after 5 hours and 15 hours.

In Fig. 7, the upper Fig.7(a) shows the status changes of the battery energy storage system within the day (15-minute interval). The SOC (State of Charge) fluctuates throughout the day, with peak and valley values occurring at noon and night, respectively. The safety risk is higher at low SOC levels. Fig. 7(b) below shows the change in SOC for weekly optimization (1-hour interval), where SOC gradually decreases during the week, reaching its lowest value on weekends, and safety risks increase as SOC approaches trough values. These analyses help to understand the operating characteristics and safety risks of batteries at different time scales.

In Fig. 8, the left diagram illustrates the power generation output of the energy system at various time scales (day-ahead, intraday, real-time, and emergency), where the real-time power generation output fluctuates significantly and the emergency power generation increases substantially during a specific time period. The figure on the right shows the power generation share and safety risk index of each energy type in different time periods. Among them, wind energy has the highest power generation share in the fourth period, and the risk index reaches the highest value of 0.28 in the sixth period. These data help to understand the operating characteristics and risk distribution of energy systems at different time scales.

In Fig. 9, the left panel displays the risk index distribution for different operating modes. The base case has a median risk index of approximately 0.3, while the maintenance model exhibits the highest risk index, with a median of approximately 0.5. The right panel shows the distribution of the energy efficiency index for different operating modes, with the base case and peak mode having the highest median energy efficiency index of approximately 0.7, while the maintenance mode has the lowest median energy efficiency index of approximately 0.6. These data indicate that the operating

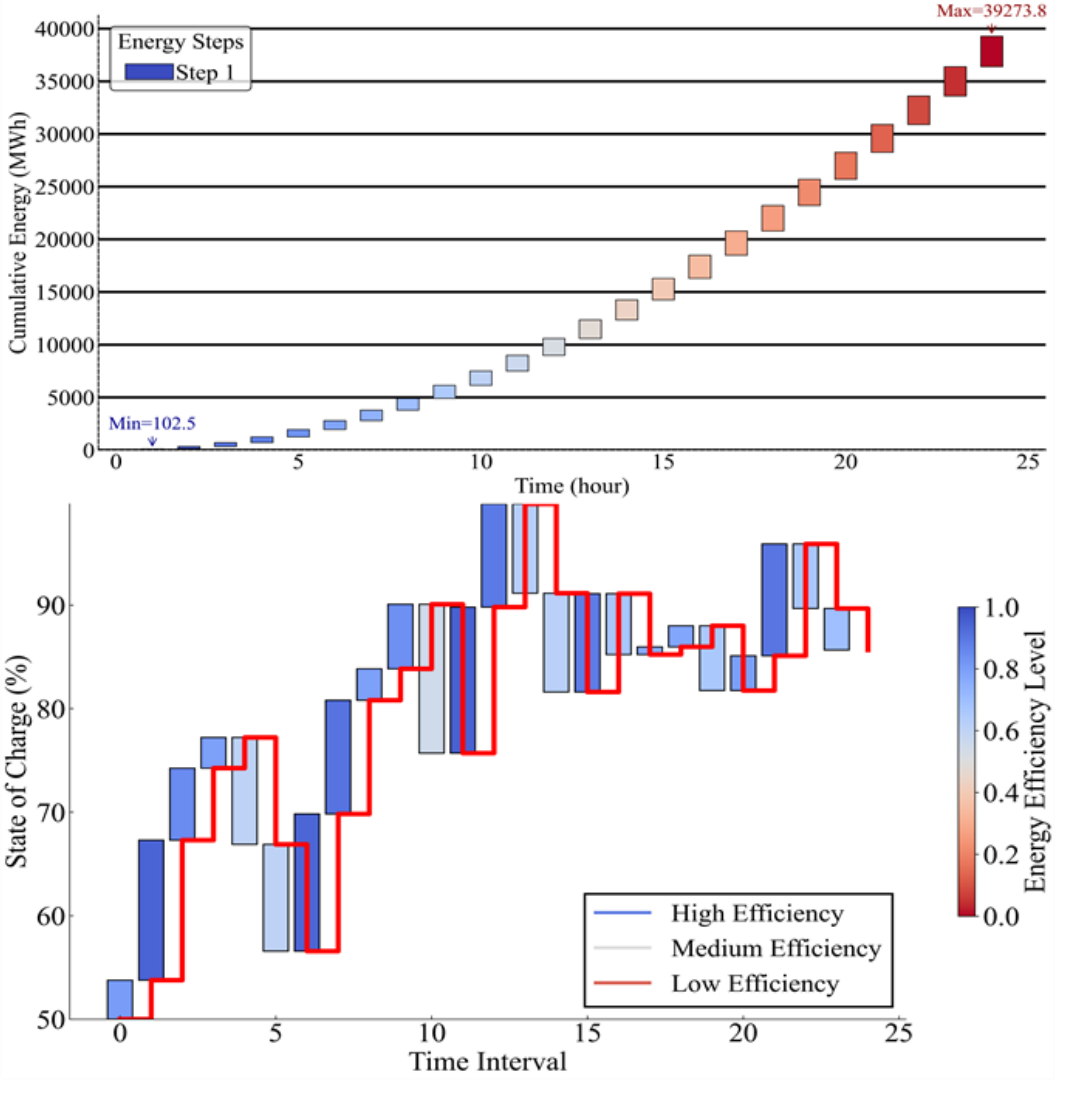

Fig. 6: Battery charge-discharge efficiency and energy accumulation analysis chart.

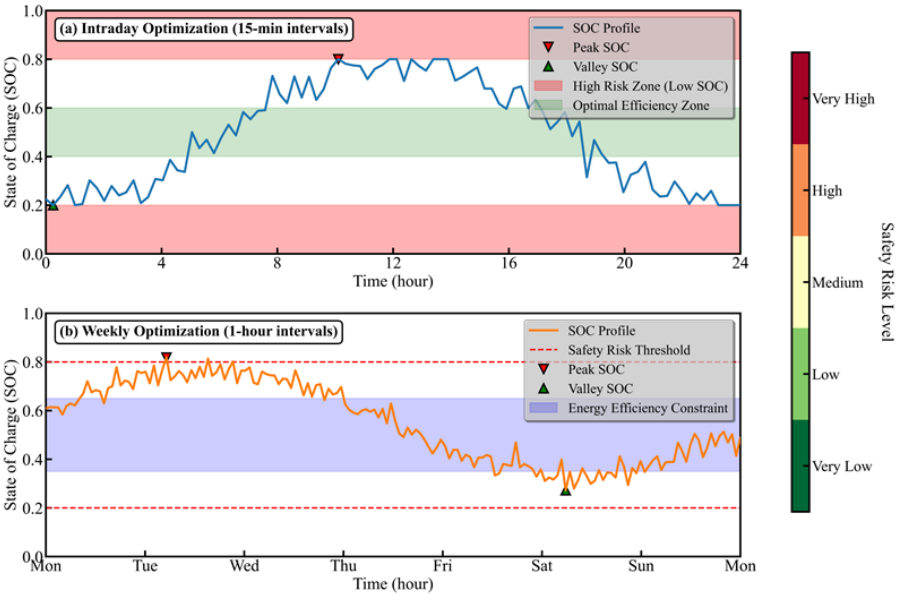

Fig. 7: Optimization analysis of charge and discharge state of battery energy storage system.

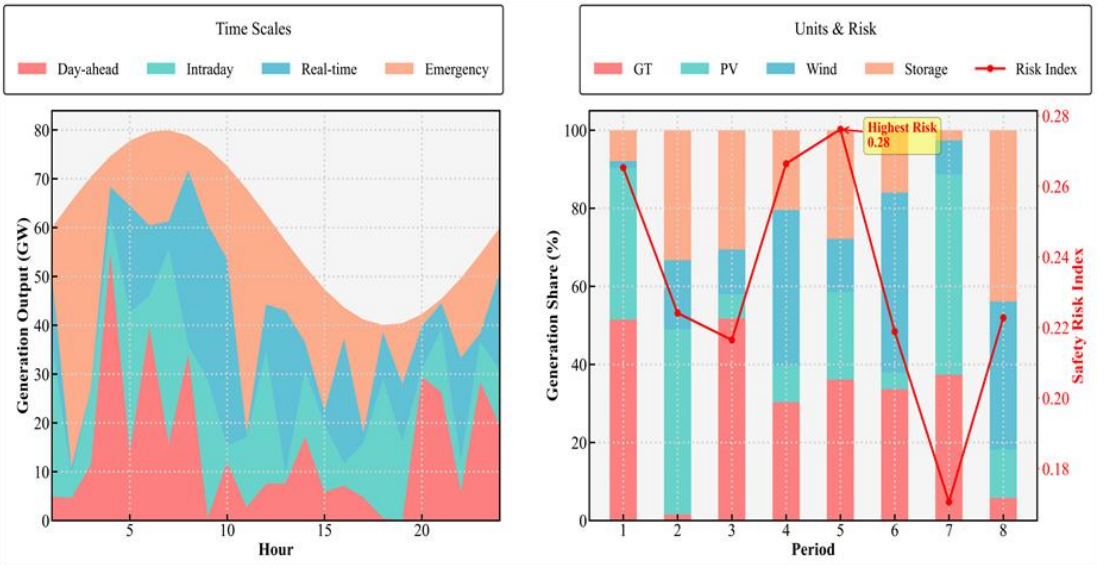

Fig. 8: Power generation output and risk analysis of energy system at different time scales.

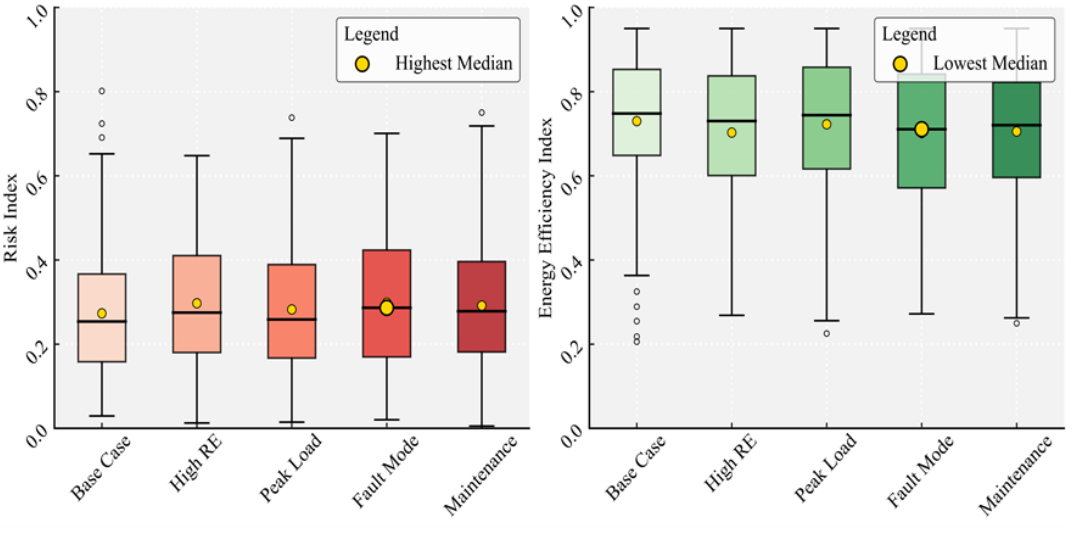

Fig. 9: Analysis of risk index and energy efficiency index under different operating modes.

mode has a significant impact on the risk and energy efficiency of the system.

In Fig. 10, the upper left figure shows the relationship between charging and discharging efficiency and C rate under different equipment safety margin (ESM) conditions, where the equipment operates most safely when ESM = 0.90. The upper right graph illustrates charge loss, discharge loss, and total round-trip loss at various C rates, with total loss increasing as the C rate increases. The figure below compares the actual power value and the predicted value for one day. The maximum error is 1.57 MW, and the 95% confidence interval shows that the prediction model has high accuracy. These analyses help optimize equipment operation and improve prediction accuracy.

In Fig. 11, the left diagram analyzes the relationship between the energy efficiency level and the safety risk index. The maximum benefit point is located at approximately 0.8 efficiency, and the risk index is 0.4. The figure on the right shows the relationship between the coordination benefit index and the system reliability. The maximum reliability is 0.97, and the corresponding coordination benefit index is about 100. These data indicate that enhancing energy system efficiency and coordination can mitigate risks and improve reliability.

Fig. 12 shows the variation of integrated energy output over different time periods. The upper left subplot shows the fluctuation in energy output from 0 to 2 hours, with a peak of around 200 kW, followed by a rapid decline below 50 kW. The subgraph in the upper right corner displays the energy output from 8 to 10 hours, exhibiting a similar fluctuation trend with a peak value that is similarly close to 200 kW. The bottom sub-diagram synthesizes data from multiple time points and illustrates the overall trend in energy output. Different colors represent the output at different time points. The overall fluctuation is small, and the energy output is relatively stable, maintaining at around 50 kW. These data suggest that the energy output has significant fluctuations in specific time periods and is more flat in other time periods.

Fig. 13 shows the relationship between energy output and device safety at different operating times. The blue dotted line represents low-risk and low-efficiency strategies, the red dotted line represents high-risk and high-efficiency strategies, and the green bar chart represents balanced backup strategies.

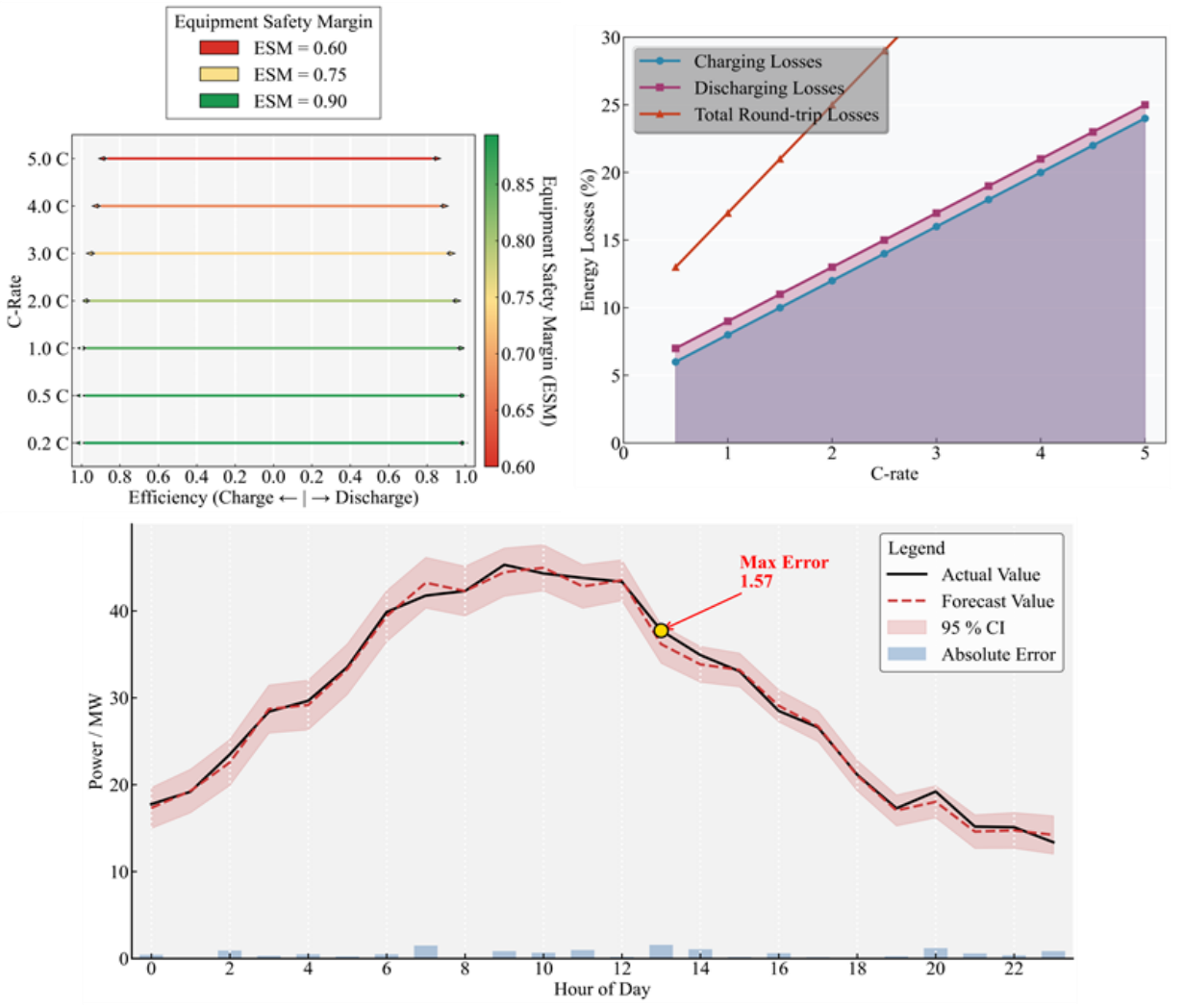

Fig. 10: Analysis of equipment safety margin and power prediction error.

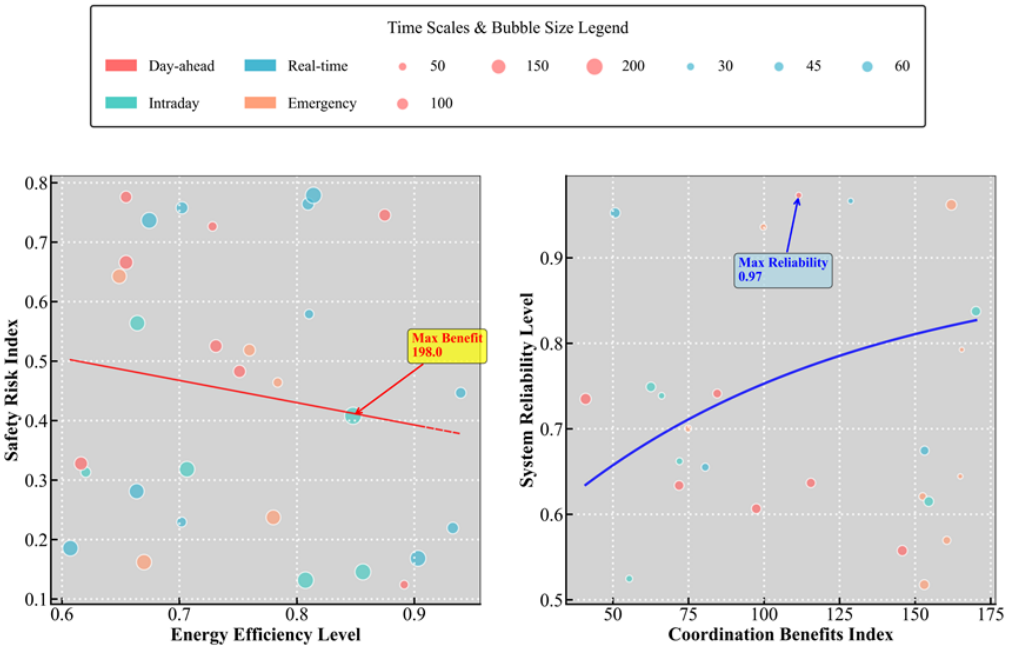

Fig. 11: Energy system efficiency, risk and coordination benefit analysis.

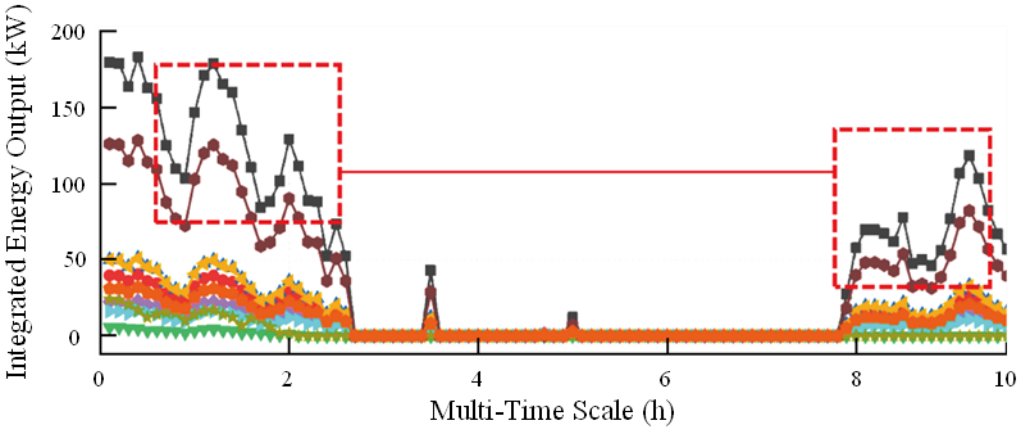

Fig. 12: Integrated energy output analysis at multiple time scales.

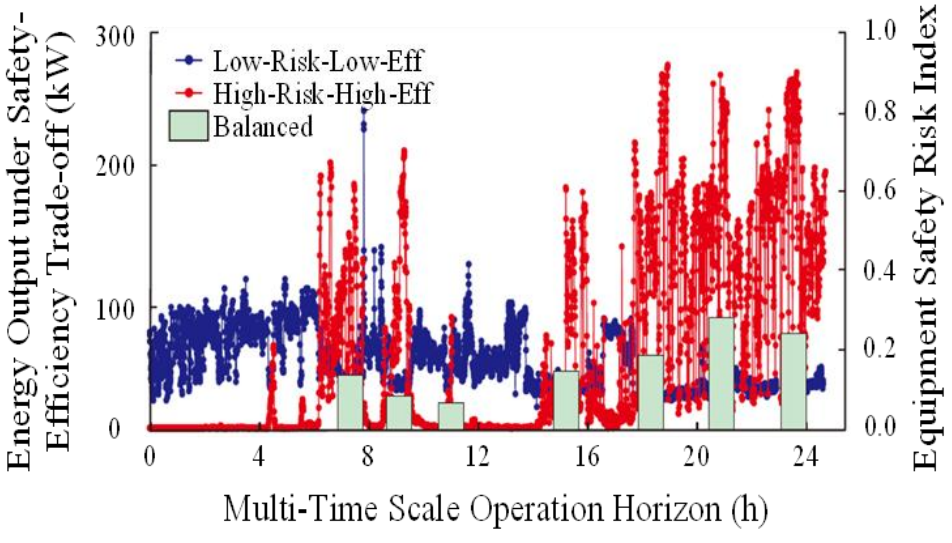

Fig. 13: Energy output and equipment safety analysis under multiple time scales.

The experimental data showed that the energy output of the low-risk strategy was stable at around 100 kW during the operation cycle of 0 to 24 hours, and the equipment safety index was close to 1.0; The energy output of the high-risk strategy fluctuates greatly, peaking up to 300 kW, but the equipment safety index is low, ranging from about 0.4 to 0.8; The energy output of the balancing strategy is between the two, and the equipment safety index is relatively stable, between 0.6 and 0.8.

5. Conclusion

This paper proposes a multi-time-scale optimization strategy for the optimal operation of Integrated Energy Systems (IES) during the energy transition.

The strategy integrates energy utilization rate with risk probability quantification through energy efficiency-safety collaborative evaluation indicators, balancing efficiency gains with equipment safety risks. A dynamic safety constraint model adjusts operational boundaries in real-time based on equipment status, ensuring safe operation. The rolling optimization algorithm combines day-ahead planning, intraday adjustments, and real-time feedback to enhance system adaptability.

Using actual IES data from a specific area, simulations show significant improvements over the benchmark method: the energy efficiency index increased by 12.8% (from 85% to 97.8%), the equipment safety risk rate decreased by 15.3% (from 10% to 8.47%), energy costs were reduced by 14.5%, and system reliability reached 96.2%. These results validate the strategy's effectiveness and support robust IES operation. Through simulation analysis, this strategy reduced carbon emissions by an average of 15% on the test set, equivalent to a reduction of approximately 1,000 tons of CO_2 per year. This is mainly due to the optimization algorithm's efficient use of renewable energy and balanced distribution of equipment load.

The proposed multi-time-scale optimization strategy effectively enhances IES energy efficiency and safety, reduces operating costs, and improves reliability. It provides a viable solution for optimizing IES operation during the energy transition, contributing to the goal of carbon neutrality.

Acknowledgments

The work was financially supported by Science and Technology Projects from State Grid Corporation of China, (Research and demonstration of multi-agent collaboration and interaction technology for urban regional integrated energy system to strengthen grid resilience, No.:5400-202317577A-3-2-ZN).

Conflict of Interest

All authors declare that they have no conflict of interest.

Supporting Information

Not applicable.

CRediT Statement

Zhenlan Dou: Write the original draft. **Chunyan Zhang:** Data collection. **Songcen Wang:** Computer simulation. **Limin Hong:** Formal analysis, Validation. **Yingying Mao:** Data curation, Visualization. **Dejian Yang:** Review & editing, Supervision. All authors read and approved the final manuscript.

References

[1] X. Zhao, X. Li, Q. Zhao, B. Yan, Y. Shi, J. Kang, Integrated model and automatically designed solver for power system restoration, *Applied Soft Computing*, 2025, **169**, 112525, doi: 10.1016/j.asoc.2024.112525.

[2] Z. Su, G. Zheng, G. Wang, M. Hu, L. Kong, An IDBO-optimized CNN-BiLSTM model for load forecasting in regional integrated energy systems, *Computers and Electrical Engineering*, 2025, **123**, 110013, doi: 10.1016/j.compeleceng.2024.110013.

[3] S. B. Tibude, G. N. Goyal, S. B. Bodkhe, A. Ranjan, Concerning energy management and optimization strategies: Deep dive into electric and hybrid vehicles: Implicit framework of machine learning, hybrid energy systems, and thermal control, *Computers and Electrical Engineering*, 2025, **127**, 110585, doi: 10.1016/j.compeleceng.2025.110585.

[4] F. Bayat, A. Roozbahani, S. M. Hashemy Shahdany, An integrated risk-based water-food-energy nexus assessment framework for surface water operation governance, *Computers and Electronics in Agriculture*, 2025, **229**, 109659, doi: 10.1016/j.compag.2024.109659.

[5] X. Yi, L. Tang, R. Cheng, M. Yin, Y. Zheng, Domain ontology to integrate building-integrated photovoltaic, battery energy storage, and building energy flexibility information for explicable operation and maintenance, *Computers in Industry*, 2025, **166**, 104250, doi: 10.1016/j.compind.2025.104250.

[6] Q. Ou, M. Yang, J. Kong, Y. Yang, Two-hop delay-aware energy efficiency resource allocation in space-air-ground integrated smart grid network, *Computers, Materials & Continua*, 2025, **83**, 2429-2447, doi: 10.32604/cmc.2025.062067.

[7] Q. Lv, J. Du, Y. Chen, R. Chen, X. Li, Effective multiparameter estimation in SIMO-OTFS system for integrated sensing and communication *via* tensor analysis, *Digital Signal Processing*, 2025, **167**, 105437, doi: 10.1016/j.dsp.2025.105437.

[8] Y. G. Son, S.-Y. Kim, Sequential constrained optimization for multi-entity operation of integrated electricity-gas distribution systems, *Energy and AI*, 2025, **22**, 100619, doi: 10.1016/j.egyai.2025.100619.

[9] C. Yuan, X. Lin, W. Zhong, Physics-embedded graph learning unlocks integrated energy system modeling, *Energy and AI*, 2025, **21**, 100597, doi: 10.1016/j.egyai.2025.100597.

[10] M. Kim, C. Joo, J. Lim, S. Yeom, I. Moon, M. Qi, J. Kim, Novel inverse predictive system integrated with industrial lubricant information, *Engineering Applications of Artificial Intelligence*, 2025, **142**, 109853, doi: 10.1016/j.engappai.2024.109853.

[11] Z. Zhang, Y. Xu, Y. Yu, X. Chen, H. Liao, Stochastic multiple

criteria decision-making for configuration selection of electricity-hydrogen integrated energy systems with multiple stakeholder interest coordination, *Engineering Applications of Artificial Intelligence*, 2025, **157**, 111323, doi: 10.1016/j.engappai.2025.111323.
[12] A. A. Mahmoud, K. Sayed, A. Daraz, Y. Arya, M. Khamies, PO-optimized cascaded FOIAN-PTD strategy for frequency control of wind-PV-thermal power system with energy storage systems, *Engineering Science and Technology, an International Journal*, 2025, **70**, 102173, doi: 10.1016/j.jestch.2025.102173.
[13] U. Subramaniam, S. Saravanan, K. R. M. Vijayachandrakala, S. Selvam, PV-integrated coordinated control for enhanced grid performance in next-gen EV charging systems, *Engineering Science and Technology, an International Journal*, 2025, **70**, 102176, doi: 10.1016/j.jestch.2025.102176.
[14] H. Zhang, I. E. Grossmann, K. McKinnon, B. R. Knudsen, R. G. Nava, A. Tomasgard, Integrated investment, retrofit and abandonment energy system planning with multi-timescale uncertainty using stabilised adaptive Benders decomposition, *European Journal of Operational Research*, 2025, **325**, 261-280, doi: 10.1016/j.ejor.2025.04.005.
[15] X. Zhang, N. Zhou, J. Liao, Q. Wang, Y. Zhou, X. Xu, E. Pouresmaeil, Flexible interconnected support for decarbonizing local energy systems with high penetration distributed energy resources and electric vehicles, *International Journal of Electrical Power & Energy Systems*, 2025, **170**, 110850, doi: 10.1016/j.ijepes.2025.110850.
[16] B. Zhou, J. He, B. Li, Y. Li, Y. Li, R. Cao, A novel fault analysis method considering control states for MMC grid-forming system with renewable energy generation, *International Journal of Electrical Power & Energy Systems*, 2025, **171**, 111031, doi: 10.1016/j.ijepes.2025.111031.
[17] X. Zhu, S. Liu, Y. Cao, Y. Zhang, An asymmetric Nash bargaining based day-ahead distributed energy sharing strategy for integrated energy service providers, *International Journal of Electrical Power & Energy Systems*, 2025, **169**, 110744, doi: 10.1016/j.ijepes.2025.110744.
[18] F. Babaei, R. B. Boozarjomehry, Z. K. Ravandi, M. R. Pishvaie, An information integration framework toward cross-organizational management of integrated energy systems, *Journal of Industrial Information Integration*, 2025, **44**, 100791, doi: 10.1016/j.jii.2025.100791.
[19] F. Khalifa, M. Marzouk, Integrated blockchain and Digital Twin framework for sustainable building energy management, *Journal of Industrial Information Integration*, 2025, **43**, 100747, doi: 10.1016/j.jii.2024.100747.
[20] T. Zhao, Z. Yan, H. Liu, B. Zhang, R. Pan, J. Xiao, F. Jiang, S. Chen, Integration of direct energy deposition systems with an optimized process planning algorithm, *Journal of Industrial Information Integration*, 2025, **46**, 100875, doi: 10.1016/j.jii.2025.100875.
[21] K. Dharani Sree, P. Karpagavalli, Enhancing the performance of power distribution systems through integrated network reconfiguration and distributed generation design, *Knowledge-Based Systems*, 2025, **330**, 114512, doi: 10.1016/j.knosys.2025.114512.
[22] L. Dong, J. Zuo, Vibration-adaptive energy management technology for self-sufficient wireless ECP braking systems on heavy-haul trains, *Mechanical Systems and Signal Processing*, 2025, **223**, 111940, doi: 10.1016/j.ymssp.2024.111940.
[23] Z. Sun, J. Hu, Z. Yao, Active vibration suppression for integrated electric drive systems based on the CNN-LSTM considering dead zone, *Mechanical Systems and Signal Processing*, 2025, **224**, 112153, doi: 10.1016/j.ymssp.2024.112153.
[24] Y. Yang, Z.-D. Xu, X.-H. Huang, P.-P. Liu, J. Dai, Y. S. Xu, Y.-R. Dong, Y. Zhang, Cross-scale integrated optimization of control system with multiple MR dampers for spatial torsional vibration mitigation, *Mechanical Systems and Signal Processing*, 2025, **229**, 112514, doi: 10.1016/j.ymssp.2025.112514.
[25] J. Li, D. Li, Y. Yang, H. Xi, W. Yu, Y. Xiao, Q. Yang, Zero-shot load forecasting for integrated energy systems: a large language model-based framework with multi-task learning, *Neurocomputing*, 2025, **654**, 131288, doi: 10.1016/j.neucom.2025.131288.
[26] J. Wang, Y. Li, Y. Hong, Y. Tang, Integrated adaptive communication in multi-agent systems: Dynamic topology, frequency, and content optimization for efficient collaboration, *Neurocomputing*, 2025, **617**, 129068, doi: 10.1016/j.neucom.2024.129068.
[27] M. A. Choukali, S. Mirbolouk, M. Valizadeh, M. C. Amirani, Deep contextual bandits-based energy-efficient beamforming for integrated sensing and communication, *Physical Communication*, 2025, **68**, 102576, doi: 10.1016/j.phycom.2024.102576.
[28] H. H. Kha, P. V. Quyet, Multi-objective optimization for active IRS-aided multi-group multicast systems with energy harvesting, integrated sensing and communication, *Physical Communication*, 2025, **69**, 102549, doi: 10.1016/j.phycom.2024.102549.
[29] J. Li, Z. Li, M. Huang, G. Huang, G. Yang, Vehicle positioning method based on UAV assisted RIS integrated sensing and communication system, *Physical Communication*, 2025, **72**, 102780, doi: 10.1016/j.phycom.2025.102780.